

<http://www.pjbs.org>

**PJBS**

ISSN 1028-8880

**Pakistan  
Journal of Biological Sciences**

**ANSI***net*

Asian Network for Scientific Information  
308 Lasani Town, Sargodha Road, Faisalabad - Pakistan



## Research Article

# Structural Insights into the Enzymatic Activity of Cysteine Protease Bromelain of MD2 Pineapple

Rafida Razali, Vijay Kumar and Cahyo Budiman

Biotechnology Research Institute, Universiti Malaysia Sabah, 88400 Kota Kinabalu, Sabah, Malaysia

## Abstract

**Background and Objective:** The MD2 pineapple contains 14 various sizes of bromelain (MD2-bromelains) ranging from 19-200 kDa which are suspected to be structurally and enzymatically varied. This study aims to compare the enzymatic activity and structural features of small and medium-sizes of MD2-bromelains, designated as MD2-SBro (19 kDa) and MD2-MBro (38 kDa), respectively. **Materials and Methods:** Purified recombinant MD2-SBro and MD2-MBro obtained were used in this study. The enzymatic activity of both MD2-bromelain was determined using a plate agar system with casein as a substrate. Three-dimensional (3D) structures of both MD2-bromelains were constructed under SWISS-MODEL server-based structural homology modeling and verified stereo-chemically. **Results:** The MD2-SBro and MD2-MBro were shown to be enzymatically active toward casein with MD2-MBro exhibited higher enzymatic activity than MD2-SBro. The 3D structures revealed that Cys-His active site position of MD2-SBro was found to be located in the inappropriate location for catalysis. Besides, the substrate-binding pocket of MD2-SBro was found to be less hydrophobic than that of MD2-MBro. **Conclusion:** Unique structural features around the active site of MD2-SBro and MD2-MBro might account for the discrepancy in their enzymatic activities.

**Key words:** Bromelain, cysteine protease, structural homology modelling, casein, SWISS MODEL

**Citation:** Rafida Razali, Vijay Kumar and Cahyo Budiman, 2020. Structural insights into the enzymatic activity of cysteine protease bromelain of MD2 pineapple. Pak. J. Biol. Sci., 23: 829-838.

**Corresponding Author:** Cahyo Budiman, Biotechnology Research Institute, Universiti Malaysia Sabah, 88400 Kota Kinabalu, Sabah, Malaysia  
Tel: +6088320000 Ext. 5350 Fax: +608832993

**Copyright:** © 2020 Rafida Razali *et al.* This is an open access article distributed under the terms of the creative commons attribution License, which permits unrestricted use, distribution and reproduction in any medium, provided the original author and source are credited.

**Competing Interest:** The authors have declared that no competing interest exists.

**Data Availability:** All relevant data are within the paper and its supporting information files.

## INTRODUCTION

Bromelain is a complex mixture of proteases mainly found in the stems and fruits of pineapple (*Ananas comosus*). Apart from the stems and fruits, bromelain was also reported to be present in pineapple peel, core, crown and leaves, with the highest proteolytic activity and protein contents detected in the extract of pineapple crown<sup>1</sup>. The biological function of bromelain for pineapple plants remains conflicting, nevertheless, it is believed to follow the main roles of the cysteine proteases in plants. In plants, cysteine proteases are known to play an important role in the growth and development and accumulation and mobilization of storage proteins such as in seeds. Besides, this group of enzyme is also known to be involved in signaling pathways and response to biotic and abiotic stresses<sup>2</sup>.

Along with papain, perhaps bromelain is the most widely known proteases in terms of traditional knowledge. This protease has been widely used as a traditional meat tenderizer for a long time due to the ability of bromelain in breakdown meat myofibril proteins<sup>3,4</sup>. In addition, bromelain has also reported exhibiting a wide range of therapeutic applications including reversible inhibition of platelet aggregation, sinusitis, surgical traumas, thrombophlebitis, pyelonephritis angina pectoris, bronchitis and enhanced absorption of drugs, particularly of antibiotics<sup>5,6</sup>. A study on oral delivery of this enzyme had also shown that this enzyme can be absorbed in human intestines and also within the gastrointestinal tract of mice without degradation and without losing its biological activity<sup>7-9</sup>.

This enzyme belongs to a cysteine protease family member with a wide range of applications. Cysteine protease is a group of protease which is characterized by the triad catalytic site of Cys-His-Asn/Glu and widely found in plant species<sup>10</sup>. The catalytic mechanism of cysteine protease was extensively studied whereby deprotonation of the thiol group of Cys by His promoted the S atom of the group become nucleophilic which further attacks the C-N bond of the substrate<sup>11</sup>.

The recent whole-genome sequence of MD2 pineapple, the most planted and popular pineapple variant in Malaysia, disclosed the presence of 14 genes encoding cysteine proteases in this pineapple variant<sup>12</sup>. The theoretical sizes of the proteins from these genes were varied, ranging from less than 19 kDa and more than 200 kDa<sup>12</sup>. It remains an open question whether these bromelains exhibit similar catalytic properties. Besides, whether all these bromelains are really required by pineapple for its biological function also remains

unclear. Unfortunately, all of the reports were only focused on the bromelain with the size of about 20-40 kDa, so-called medium-sized bromelain<sup>13,14</sup>. No report for the bromelain with a size of less than 20 kDa (small-sized bromelain).

This report provides the first evidence on comparative analysis of the enzymatic activity of small- and medium-sized bromelain of MD2 pineapple, designated as MD2-SBro and MD2-MBro, respectively. Insight into the three-dimensional structures of MD2-SBro and MD2-MBro were also provided to address the issues on their enzymatic activity differences.

## MATERIALS AND METHODS

**Study area:** The experiment was carried out at Biotechnology Research Institute, Universiti Malaysia Sabah in accordance with the institute guidelines and regulations from January, 2018-July, 2019.

**Chemicals:** All chemicals were purchased from Nacalai Tesque, Inc. (Kyoto, Japan) and used without further purification unless otherwise stated.

**Protein:** The protein used in this study was purified recombinant full-length of MD2-SBro and MD2-MBro which contain glutathione-S-transferase and thioredoxin tags, respectively, at their N-terminal. Prior to the analysis, the purity of the proteins was checked using a 15% gel of SDS-PAGE. To remove aggregated proteins and other particles, the sample was centrifuged at 30,000 g for 30 min at 4°C followed by filtration of the supernatant using 0.22 µm filters (Millipore Corp., Bedford, MA).

**Enzymatic activity:** The plate agar system was used to check the proteolytic activity of the pure proteins. This was determined by the well diffusion method according to Vijayaradhavan and Vincent<sup>15</sup> with some modifications. The casein plates containing 2% casein in a solution of 1.5% of bacto agar were prepared. The media was adjusted to pH 7.0 and sterilized (121°C). Prior to the pouring of the media into the sterilized petri dish, antibiotic was added into the media when its temperature has reached 50°C. The media was then poured and solidified for 30 min. The wells were then made on the solidified casein agar plates. The degradation of the casein substrate in the plate was then performed by loading the pure proteins and sterilized distilled water (control) into each well and observing the formation of the halo zone around the well. These plates were incubated 24 h at 37°C.

**Structural homology modeling:** The amino acid sequences of MD2-SBro and MD2-MBro were retrieved from NCBI with the accession numbers of OAY85828.1 and OAY85858.1, respectively. These sequences were used as targets for homology modeling using the SWISS-MODEL server<sup>16,17</sup> and generating the 3D models for all target sequences. The finest generated 3D model structures were then visualized using PyMOL software. The structures were validated according to Global Model Quality Estimation (GMQE), QMEAN<sup>18,19</sup> and Ramachandran plot<sup>20</sup>. The query coverage and percent identity of the models with the templates were also identified using the SWISS-MODEL<sup>21</sup>. The degree of structural similarity between the 3D models of MD2-SBro and MD2-MBro and the templates selected by SWISS-MODEL server, with other well-characterized plant cysteine proteases was calculated by PyMOL software which measured the root-mean-square deviation (RMSD) between these two superimposed proteins, respectively.

**Identification active sites:** The identification of the MD2-SBro and MD2-MBro active site residues was carried out by doing multiple sequence alignments using T-Coffee<sup>22-25</sup>. The sequence comparison was done with other well-characterized plant cysteine proteases. The three residues of MD2-SBro or MD2-MBro that correspond well to the triad catalytic sites of the other cysteine protease were then designated as the active site residues (catalytic triad) of these two bromelains. The position and distance of the active site residues between each other were also identified and calculated. Surface charge analysis of the substrate-binding pocket of MD2-SBro and MD2-MBro were then analysed according to Eisenberg *et al.*<sup>26</sup> All results were visualized under PyMOL software.

**Statistical analysis:** The data of clear zone diameter were shown as a mean  $\pm$  standard of deviation from three independent replications and descriptively analyzed.

## RESULTS

**Protein:** The proteins used in this study were obtained from the heterologous expression system under *Escherichia coli* BL21 (DE3) system. The purity of the proteins was considerably high (Fig. 1) hence, acceptable for enzymatic analysis. The apparent size of MD2-SBro and MD2-MBro were 46 and 56 kDa in 15% SDS-PAGE, respectively. These sizes were higher than their theoretical sizes (19 kDa for MD2-SBro and 38 kDa for MD2-MBro) due to the presence of GST-tag (26 kDa) or Trx-tag (12 kDa). Noteworthy, MD2-SBro is the smallest bromelain found in MD2-pineapple.

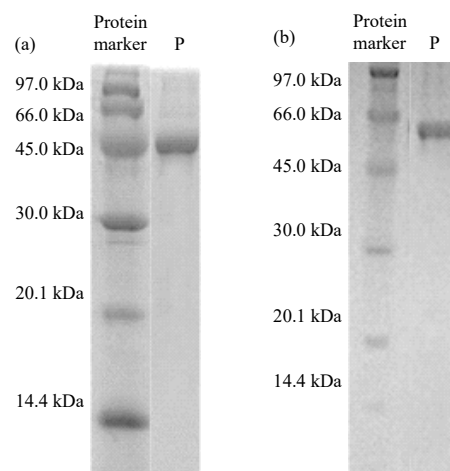


Fig. 1(a-b): Purified (a) MD2-SBro and (b) MD2-MBro

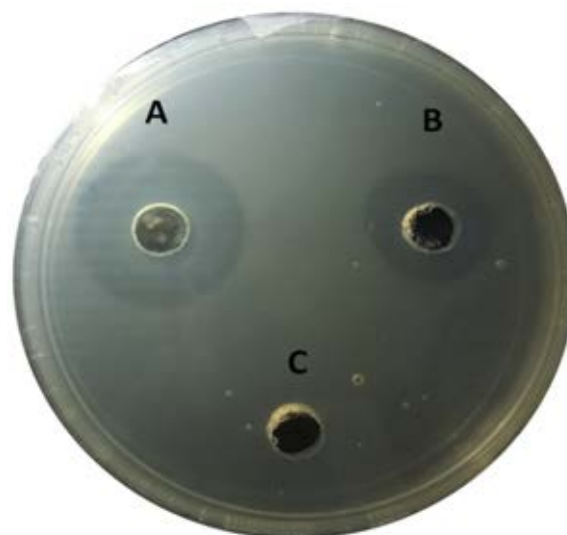


Fig. 2: Halo zone formed on casein plate agar by purified MD2-SBro (well A) or MD2-MBro (Well B) after 24 h incubation at 37°C. The negative control (buffer) is shown in well C

Protein concentration used in this experiment was 0.1 mg mL<sup>-1</sup>

**Catalytic activity:** The clear zone was detected on the casein agar plate in determining protease activity. The clear zone observed on the plate for both MD2-bromelain pure proteins after an overnight incubation (Fig. 2). The halo zone for MD2-MBro has shown to be remarkably wider (diameter size: 2.6  $\pm$  0.1 cm) than that of MD2-SBro (diameter size: 2.0  $\pm$  0.08 cm). No clear zone was observed in the negative control (buffer).

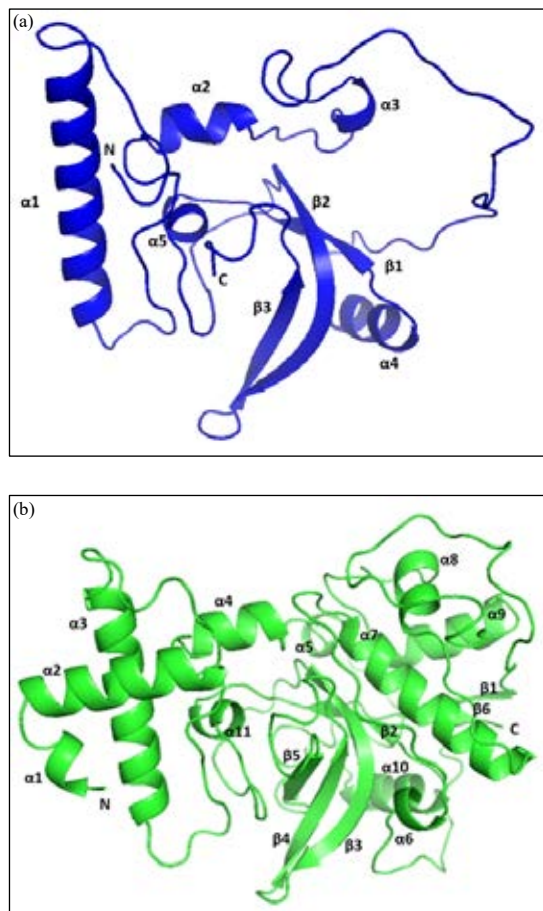


Fig.3(a-b): Three-dimensional model of (a) MD2-SBro and (b) MD2-MBro obtained from structural homology modeling

Table 1: Structural validation and stereo-chemical analysis of MD2-bromelain models

Models	MD2-SBro	MD2-MBro
Global model quality estimation (GMQE)	0.74	0.46
QMEAN z-score	-2.93	-2.00
<b>Ramachandran plot</b>		
Favoured region (%)	92.30	95.20
Allowed region (%)	7.10	3.80
Outlier region (%)	0.60	1.00

### Structural homology modeling

**Structural validation:** Three models (models 01, 02 and 03) were produced by SWISS-MODEL for each MD2-SBro and MD2-MBro. Nevertheless, structural validation and assessment (Table 1) revealed that only models 01 was acceptable for both MD2-bromelains (Fig. 3). For structural validation, global model quality estimation (GMQE) of MD2-SBro model and MD2-MBro model was 0.74 and 0.46 out of 0-1 scale, respectively. The scores indicated that the model quality was

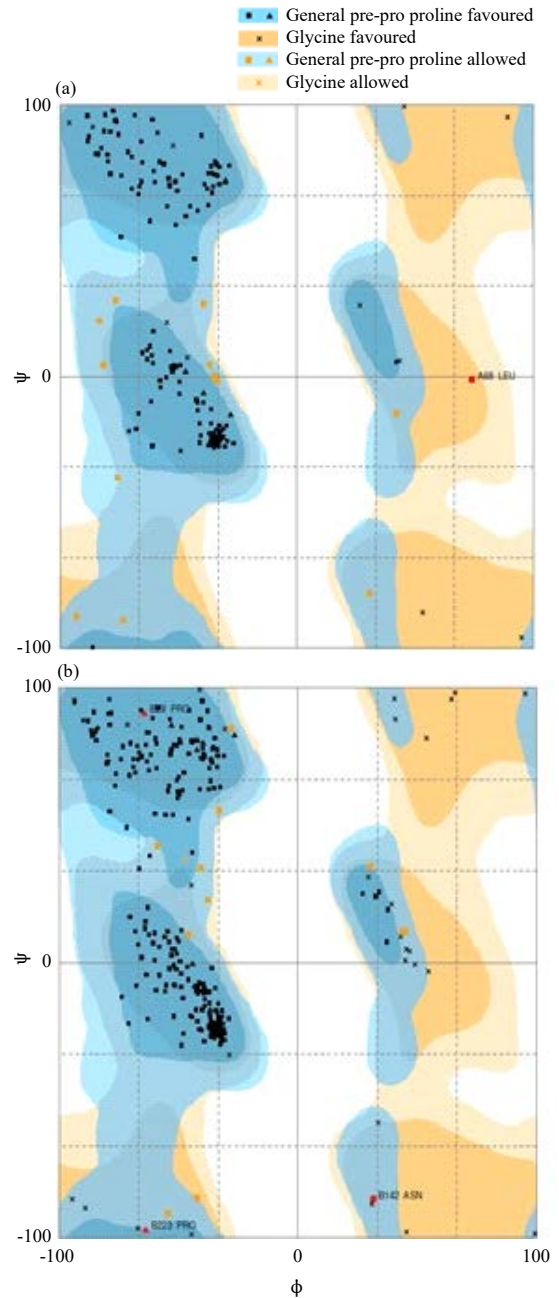


Fig.4(a-b): Ramachandran plot of the structural model of (a) MD2-SBro and (b) MD2-MBro

on a high moderate level. Furthermore, both MD2-SBro and MD2-MBro models also have a good score on the QMEAN z-score which are -2.93 and -2.00, respectively, which were higher the minimum requirement of -4.00 to be considered as a good quality model<sup>19</sup>. Further, the Ramachandran plot (Fig. 4) showed that most of the amino acids of the MD2-SBro model structure were located in the favorable region (92.3%). Meanwhile, 7.1% were in the allowed region and only 0.6%

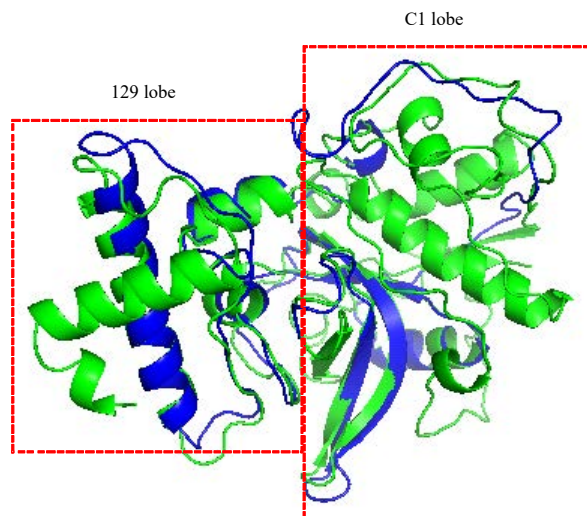


Fig. 5: Superimposed between MD2-SBro (blue) and MD2-MBro (green) structures with RMSD value of 1.26 Å

Table 2: Degree of structural similarity of MD2-bromelains with the template proteins and other cysteine proteases

Proteins	RMSD	
	MD2-SBro	MD2-MBro
Template	0.114 Å	0.132 Å
Papain	1.344 Å	0.597 Å
Cysteine protease from <i>Zingiber officinale</i> (GP-II)	0.738 Å	0.524 Å
Cathepsin B	1.025 Å	1.050 Å

(equal to 1 amino acid region) in the outlier region. The residue located in the outlier region of MD2-SBro was Leu68. Meanwhile, for MD2-MBro model structure, 95.2% of amino acid was in the favorable region (Fig. 4). The 1% of amino acid percentage (3 residues) in the outlier region were Pro29, Asn142 and Pro223. Altogether, nearly 100% of the residues for both MD2-SBro and MD2-MBro were in the favored and allowed regions. Altogether, the structural validation parameters indicated that both models were acceptable. The degree of structural similarity between the MD2-bromelains' models with other cysteine proteases, as shown in Table 2, indicated that structures are almost similar to each other. Meanwhile, the superimposition between models of MD2-SBro and MD2-MBro yielded an RMSD value of 1.26 Å with the differences in their N- and C-terminal regions, with the overall amino acid sequence identity of 65.68% (Fig. 5).

**Three-dimensional model structures:** The acceptable models of MD2-SBro and MD2-MBro were shown in Fig. 3 and 5. The structures were dominated by helical structures, whereby 5 and 11 helical segments were found in MD2-SBro and MD2-MBro models, respectively. The structures seemed to be

organized into two lobes of I29 and C1 lobes (Fig. 5). For MD2-MBro, the separation of the lobes was quite clear, whereby the first lobe involved  $\alpha 1$ ,  $\alpha 2$ ,  $\alpha 3$ ,  $\alpha 4$  and  $\alpha 11$  segments (I29 lobe), while the second lobe involved the rest of helical segments and  $\beta$ -sheet segments (C1 lobe). As for MD2-SBro, the lobe separation was not clear, nevertheless, it seemed that  $\alpha 1$ ,  $\alpha 2$  and  $\alpha 5$  segments were organized into the first lobe form, while the other segments form the second lobe.

**Active site identification:** Amino acid sequences alignment of MD2-SBro with other well-characterized cysteine proteases revealed that the His141 and Asn163 of MD2-SBro were well conserved to the His and Asn active site residues of the other cysteine protease (Fig. 6). However, none of Cys residues of MD2-SBro (Cys69, Cys79 and Cys136) were in conserved position to the Cys active site of the other cysteine proteases. Nevertheless, the structural model of M2-SBro showed that Cys69 is the closest distance to the His141 residue. Therefore, Cys69 is suspected to be the Cys active site for the MD2-SBro yielding a complete set of the catalytic triad sites consisting of Cys69, His141 and Asn163. Meanwhile, sequence alignment shown in Fig. 7 suggested that Cys147, His280 and Asn301 MBro were the catalytic triad of MD2-MBro as these residues were highly conserved with the Cys-His-Asn of the catalytic triad of the other cysteine protease. The local configuration of the catalytic triads of MD2-SBro and MD2-MBro showed that the distance between Cys69 and His141 of MD2-SBro was 7.3 Å (Fig. 8a). Meanwhile, the distance between Cys147 and His280 in MD2-MBro, which was only 3.3 Å apart (Fig. 8b). Further analysis of the substrate-binding pocket region

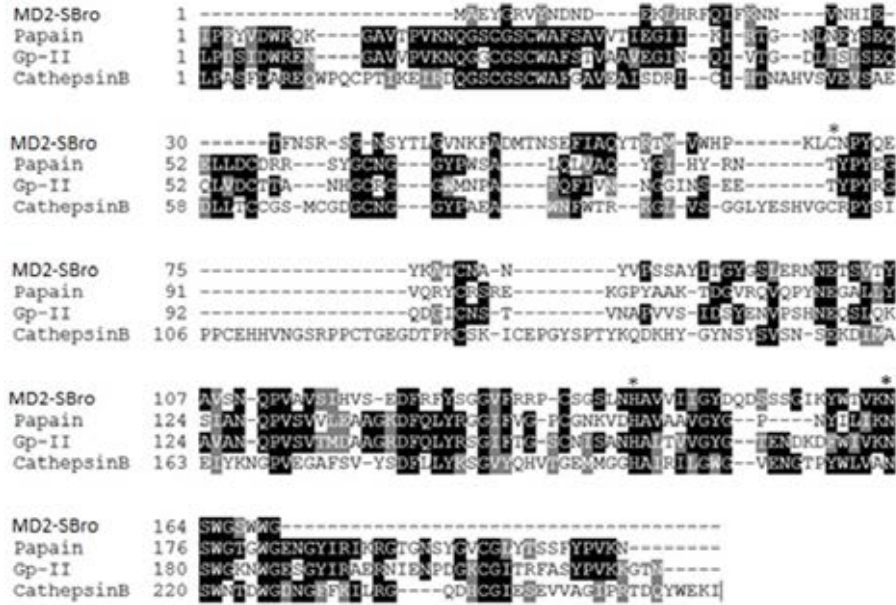


Fig. 6: Structure-based sequence alignment between MD2-SBro with other well-characterized cysteine proteases  
 Putative catalytic triad of MD2-SBro was indicated by an asterisk (\*) above the sequence

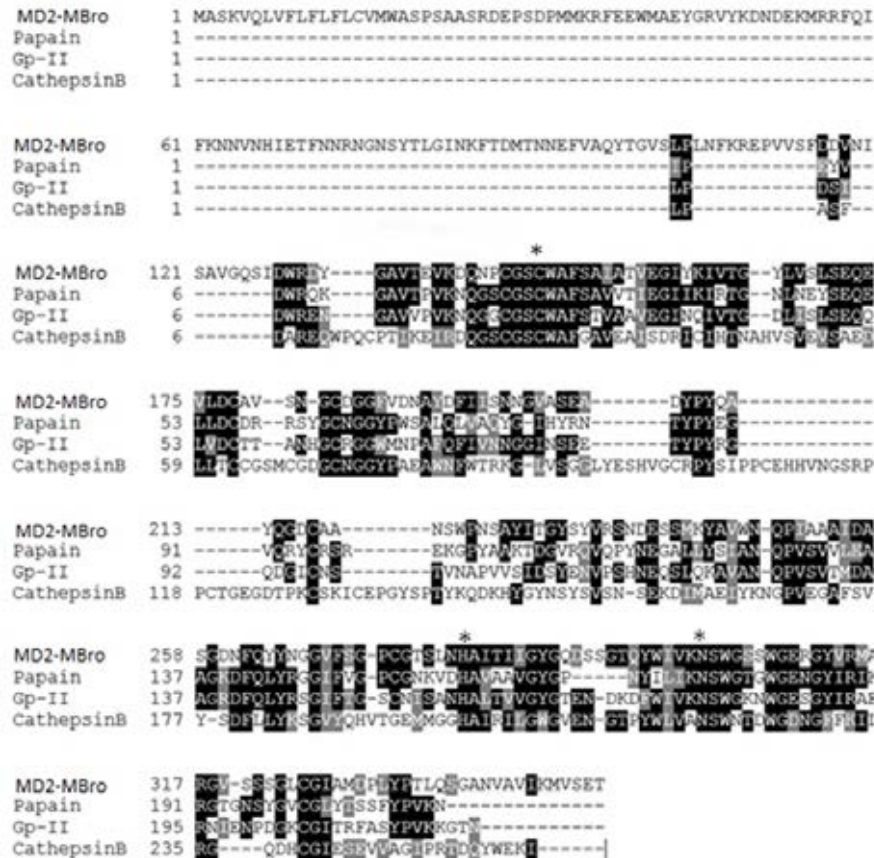


Fig. 7: Structure-based sequence alignment between MD2-MBro with other well-characterized cysteine proteases  
 Putative catalytic triad of MD2-MBro was indicated by an asterisk (\*) above the sequence

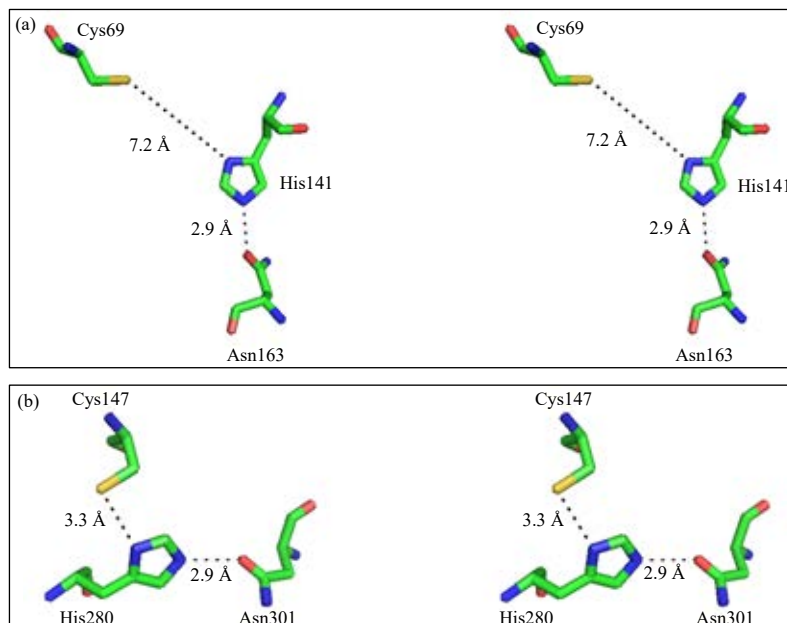


Fig. 8(a-b): Stereo view (cross-eye) of the configuration of catalytic triad residues of (a) MD2-SBro and (b) MD2-MBro

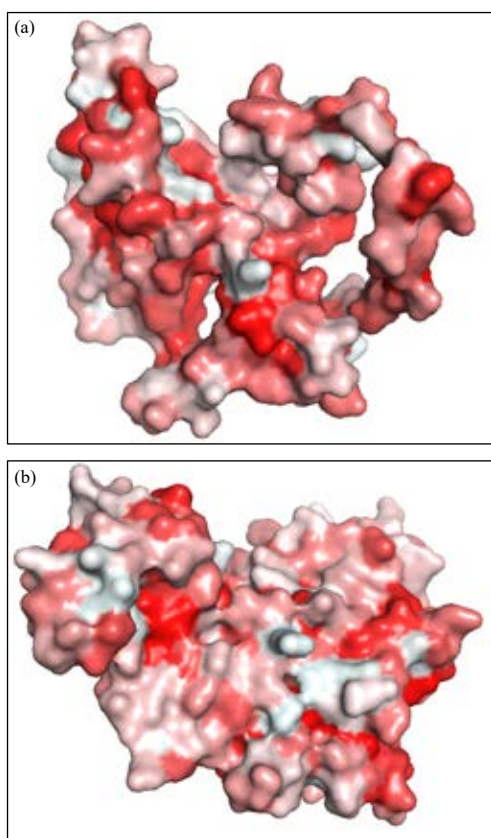


Fig. 9(a-b): Complex of (a) MD2-SBro and (b) MD2-MBro highlighted in hydrophobic (red) to non-hydrophobic (white) gradient

revealed that the substrate-binding pocket of MD2-MBro was found to be dominated by hydrophobic residues (Fig. 9). Meanwhile, the pocket of MD2-SBro was predicted to be less hydrophobic with different geometrical shape to that of MD2-MBro.

## DISCUSSION

Figure 2 clearly suggested that the enzymatic activity of MD2-MBro is considerably higher than that of MD2-SBro. Overall structures of MD2-SBro and MD2-MBro (Fig. 3) displayed domination of helical structures in the model which are in good agreement with Tap *et al.*<sup>27</sup> and Omotoyinbo *et al.*<sup>28</sup> and known to be a common feature in cysteine protease<sup>29</sup>. To note, MD2-SBro was found to be rich with a flexible region, particularly in the form of a loop, implying that this protein is structurally more flexible than MD2-MBro. Further, Fig. 3 showed that both MD2-bromelains' structures were apparently organized into two lobes. The lobe organization was also a common feature in cysteine protease, particularly for papain<sup>30</sup>. Interestingly, structural modeling of fruit and stem bromelain reported by Ramli *et al.*<sup>31</sup> also indicated the separation of the lobes (or so-called domain), which further labelled the first lobe as the I29 domain (fully composed by helical structure) and the second lobe as peptidase C1 domain. The variation among bromelain structures was usually found in the I29 domain, meanwhile, the peptidase C1 domain was found to be highly similar



among cysteine protease members<sup>31</sup>. Nevertheless, in this study, the structural alignment revealed that both domains of MD2-SBro and MD2-MBro were found to be different, which might contribute to the differences in their catalytic properties.

Further interesting structural feature was the cleft formed by these two lobes/domains. The cleft was found to be the location of the active sites for the cysteine protease and bromelain<sup>30,31</sup>. To note, while the side chains of the residues of the active site pointing out of the cleft, those residues are basically attached to the segment of the peptidase C1 domain. As the peptidase C1 domain was previously proposed to be similar among bromelain<sup>31</sup>, this might suggest that the bromelain exhibited a similar catalytic mechanism. In this study, the active sites of MD2-SBro and MD2-MBro were also found in the cleft. Nevertheless, as the peptidase C1 domains of those proteins were found to be different, the orientation of the active site of both MD2-bromelains might also be different.

It is interesting that while both MD2-SBro and MD2-MBro have conserved triad catalytic of Cys-His-Asn (Fig. 6, 7), the model structures of MD2-SBro and MD2-MBro further revealed interesting evidence that the configurations of in triad catalytic residues between both MD2-bromelains were different (Fig. 8). The distance of His141-Cys69 in MD2-SBro was considerably too far (7.3 Å) for catalysis. At this distance, MD2-SBro was supposedly enzymatically inactive. However, the fact that MD2-SBro remains active (against casein substrate), albeit low activity, might suggest that the deprotonation of Cys69 by His141 remains to occur. This might be related to the position of Cy69 in the long loop extending from Lys67 to Glu101 (Fig. 8). The loop was believed to be flexible which therefore causes the position of Cys69 to be mobile and the distance of His141-Cys69 was, therefore, dynamic. On the other side, the configuration of the catalytic triad of MD2-MBro was found to be in an appropriate distance for catalysis. To note, Cys147 of MD2-MBro was not located at the flexible loop therefore the distance of His-Cys of this protein was always in the acceptable range for the catalysis. Accordingly, the dynamic of the active site loop of MD2-SBro was believed to be responsible for its catalytic activity. Indeed, some reports suggested that the dynamic of the loop around the active site was known to be one factor affecting the catalytic activity of the enzyme<sup>32-34</sup>.

Another possibility for the differences in the enzymatic activity between MD2-SBro and MD2-MBro might be due to their substrate-binding cavity properties. As shown in Fig. 9, the region around an active site (substrate-binding cavity) of MD2-SBro was found to be more polar than MD2-MBro. To note, the casein substrate used in this study was known to be

a hydrophobic protein<sup>35</sup>. Accordingly, the substrate-binding cavity of MD2-MBro was more appropriate for the casein substrate. Besides, hydrophobicity around active sites might also involve in desolvation events during catalysis. The desolvation hypothesis was one of the widely acceptable catalysis mechanisms, whereby the enzymes remove water molecules from the reactants and created an environment similar to the gas phase for the reacting substrates<sup>36,37</sup>.

This is the first report showing that different types of bromelain from one pineapple variant exhibited different enzymatic activity. This might reflect the specificity of their biological functions. Besides, this allows us to select which type of bromelain is enzymatically suitable for certain applications.

## CONCLUSION

This study clearly indicated that the bromelain with different sizes, as evidenced by MD2-SBro and MD2-MBro, exhibited different catalytic properties. The catalytic discrepancy is associated with differences in their structural features mainly in the configuration of the catalytic triad due to the flexible loop. Besides, the differences in the hydrophobicity of the substrate-binding cavity might also contribute to the catalytic discrepancy.

## SIGNIFICANCE STATEMENT

This study discovers the enzymatic activity and structural differences of cysteine proteases bromelain of MD2 pineapple (MD2-bromelain) that can be beneficial for further studies and industrial applications. This study will help the researcher to uncover the critical areas of structural regulation in enzymatic properties of different types of bromelain that many researchers have not explored. Thus, a new theory on the mechanism by which MD2-bromelain exhibits the catalytic mechanism may be arrived at.

## ACKNOWLEDGMENT

This study was supported by GUG0104-1/2017 research grants.

## REFERENCES

1. Ketnawa, S., P. Chaiwut and S. Rawdkuen, 2012. Pineapple wastes: A potential source for bromelain extraction. *Food Bioprod. Proces.*, 90: 385-391.
2. Grudkowska, M. and B. Zagdanska, 2004. Multifunctional role of plant cysteine proteinases. *Acta Biochim. Pol.*, 51: 609-624.

3. Omojasola, P.F., O.P. Jilani and S.A. Ibiyemi, 2008. Cellulase production by some fungi cultured on pineapple waste. *Nat. Sci.*, 6: 64-79.
4. Nadzirah, K.Z., S. Zainal, A. Noriham and I. Normah, 2016. Application of bromelain powder produced from pineapple crowns in tenderising beef round cuts. *Int. Food Res. J.*, 23: 1590-1599.
5. Pavan, R., S. Jain and A. Kumar, 2012. Properties and therapeutic application of bromelain: A review. *Biotechnol. Res. Int.*, 10.1155/2012/976203
6. Rathnavelu, V., N.B. Alitheen, S. Sohila, S. Kanagesan and R. Ramesh, 2016. Potential role of bromelain in clinical and therapeutic applications (Review). *Biomed. Rep.*, 5: 283-288.
7. Chobotova, K., A.B. Vernallis and F.A.A. Majid, 2010. Bromelain's activity and potential as an anti-cancer agent: Current evidence and perspectives. *Cancer Lett.*, 290: 148-156.
8. Castell, J.V., G. Friedrich, C.S. Kuhn and G.E. Poppe, 1997. Intestinal absorption of undegraded proteins in men: Presence of bromelain in plasma after oral intake. *Am. J. Physiol.-Gastroint. Liver Physiol.*, 273: G139-G146.
9. Hale, L.P., 2004. Proteolytic activity and immunogenicity of oral bromelain within the gastrointestinal tract of mice. *Int. Immunopharmacol.*, 4: 255-264.
10. Verma, S., R. Dixit and K.C. Pandey, 2016. Cysteine proteases: Modes of activation and future prospects as pharmacological targets. *Front. Pharmacol.*, Vol. 7. 10.3389/fphar.2016.00107.
11. Hull, R., 2014. Chapter 6-Genome Composition, Organization and Expression. In: *Plant Virology*, 5th Edn., Hull, R. (Eds.), Academic Press, New York, ISBN: 978-0-12-384871-0, pp: 247-339.
12. Redwan, R.M., A. Saidin and S.V. Kumar, 2016. The draft genome of MD-2 pineapple using hybrid error correction of long reads. *DNA Res.*, 23: 427-439.
13. Arshad, Z.I.M., A. Amid, F. Yusof, I. Jaswir, K. Ahmad and S.P. Loke, 2014. Bromelain: An overview of industrial application and purification strategies. *Applied Microbiol. Biotechnol.*, 98: 7283-7297.
14. Benefo, E.O. and I.W. Ofosu, 2018. Bromelain activity of waste parts of two pineapple varieties. *Sustain. Food Prod.*, 2: 21-28.
15. Vijayaraghavan, P. and S.G.P. Vincent, 2013. A simple method for the detection of protease activity on agar plates using bromocresolgreen dye. *J. Biochem. Technol.*, 4: 628-630.
16. Biasini, M., S. Bienert, A. Waterhouse, K. Arnold and G. Studer *et al.*, 2014. SWISS-MODEL: Modelling protein tertiary and quaternary structure using evolutionary information. *Nucl. Acids Res.*, 42: W252-W258.
17. Bordoli, L., F. Kiefeer, K. Arnold, P. Benkert, J. Battey and T. Schwede, 2009. Protein structure homology modeling using SWISS-MODEL workspace. *Nat. Protoc.*, 4: 1-13.
18. Benkert, P., M. Kunzli and T. Schwede, 2009. QMEAN server for protein model quality estimation. *Nucl. Acids Res.*, 37: W510-W514.
19. Benkert, P., M. Biasini and T. Schwede, 2011. Toward the estimation of the absolute quality of individual protein structure models. *Bioinformatics*, 27: 343-350.
20. Lovell, S.C., I.W. Davis, W.B. Arendall, P.I. de Bakker and J.M. Word *et al.*, 2003. Structure validation by C $\alpha$  geometry:  $\phi$ ,  $\psi$  and C $\beta$  deviation. *Proteins: Struct. Funct. Bioinform.*, 50: 437-450.
21. Bhagavathi, S., G. Wadhwa and A. Prakash, 2012. *In silico* modelling and validation of differentially expressed proteins in lung cancer. *Asian Pac. J. Trop. Dis.*, 2: S524-S529.
22. Armougom, F., S. Moretti, Q. Poirot, S. Audic and P. Dumas *et al.*, 2006. Espresso: Automatic incorporation of structural information in multiple sequence alignments using 3D-coffee. *Nucleic Acids Res.*, 34: W604-W608.
23. Di Tommaso, P., S. Moretti, I. Xenarios, M. Orobitz and A. Montanyola *et al.*, 2011. T-Coffee: A web server for the multiple sequence alignment of protein and RNA sequences using structural information and homology extension. *Nucl. Acids Res.*, 39: W13-W17.
24. Notredame, C., D.G. Higgins and J. Heringa, 2000. T-Coffee: A novel method for fast and accurate multiple sequence alignment. *J. Mol. Biol.*, 302: 205-217.
25. O'Sullivan, O., K. Suhre, C. Abergel, D.G. Higgins and C. Notredame, 2004. 3D Coffee: Combining protein sequences and structures within multiple sequence alignments. *J. Mol. Biol.*, 340: 385-395.
26. Eisenberg, D., E. Schwarz, M. Komaromy and R. Wall, 1984. Analysis of membrane and surface protein sequences with the hydrophobic moment plot. *J. Mol. Biol.*, 179: 125-142.
27. Tap, F.M., F.A.A. Majid and N.B.A. Khairudin, 2016. Structure prediction of stem bromelain from pineapples (*Ananas comosus*) using procaricain enzyme as a modelling template. *Int. J. Applied Eng. Res.*, 11: 6109-6111.
28. Omotoyinbo, O.V., I.E. Ekpenyong, T. Hezekiah and M.D. Sanni, 2018. *In silico* evaluation of bromelain from stem and fruit of pineapple (*Ananas comosus*). *J. Agric. Sci. Food Technol.*, 4: 32-40.
29. Huet, J., Y. Looze, K. Bartik, V. Raussens, R. Wintjens and P. Boussard, 2006. Structural characterization of the papaya cysteine proteinases at low pH. *Biochem. Biophys. Res. Commun.*, 341: 620-626.
30. Kamphuis, I.G., K.H. Kalk, M.B.A. Swarte and J. Drenth, 1984. Structure of papain refined at 1.65 Å resolution. *J. Mol. Biol.*, 179: 233-256.

31. Ramli, A.N.M., N.H.A. Manas, A.A.A. Hamid, H.A. Hamid and R.M. Illias, 2018. Comparative structural analysis of fruit and stem bromelain from *Ananas comosus*. *Food Chem.*, 266: 183-191.
32. De Brevern, A.G., A. Bornot, P. Craveur, C. Etchebest and J.C. Gelly, 2012. PredyFlexy: Flexibility and local structure prediction from sequence. *Nucl. Acids Res.*, 40: W317-W322.
33. Alvarez, L., A. Lewis-Ballester, A. Roitberg, D.A. Estrin, S.R. Yeh, M.A. Marti and L. Capece, 2016. Structural study of a flexible active site loop in human indoleamine 2, 3-dioxygenase and its functional implications. *Biochemistry*, 55: 2785-2793.
34. Montagner, C., M. Nigen, O. Jacquin, N. Willet and M. Dumoulin *et al.*, 2016. The role of active site flexible loops in catalysis and of zinc in conformational stability of *Bacillus cereus* 569/H/9  $\beta$ -lactamase. *J. Biol. Chem.*, 291: 16124-16137.
35. Dalglish, D.G., 1998. Casein micelles as colloids: Surface structures and stabilities. *J. Dairy Sci.*, 81: 3013-3018.
36. Dewar, M.J.S., 1986. New ideas about enzyme reactions. *Enzyme*, 36: 8-20.
37. Wolfenden, R., 1983. Waterlogged molecules. *Science*, 222: 1087-1093.